



Assessment of vegetable wastes for basic violet 14 removal: role of sorbent surface chemistry and porosity

M. Àngels Olivella^{a,*}, Núria Fiol^b, Florencio de la Torre^b, Jordi Poch^c,
Isabel Villaescusa^b

^aFacultat de Ciències, Department of Chemistry, Universitat de Girona, Campus Montilivi s/n, 17071 Girona, Spain
Tel. +34 972418416; email: angels.olivella@udg.edu

^bDepartment of Chemical Engineering, Escola Politècnica Superior, Universitat de Girona, Avda. Lluís Santaló, s/n, 17071 Girona, Spain

^cDepartment of Applied Mathematics, Escola Politècnica Superior, Universitat de Girona, Avda. Lluís Santaló, s/n, 17071 Girona, Spain

Received 30 July 2013; Accepted 29 October 2013

ABSTRACT

In this work, two vegetable wastes (i.e. grape stalks and cork bark) have been investigated as potential sorbents for the removal of the dye basic violet 14 or commonly named basic fuchsin from aqueous solution. The physical and chemical properties of grape stalks and cork bark defined by elemental analysis, polarity index, acidic functional groups, FTIR analysis, surface area and porosity were investigated to explain the different sorption behaviour of these two sorbents towards basic fuchsin removal. Effect of solution pH on basic fuchsin sorption onto both vegetable wastes has been investigated and sorption kinetics and isotherms determined. Results have been compared to those obtained using a commercial activated carbon. Langmuir maximum sorption capacity of grape stalks (106.8 mg g^{-1}) estimated by the orthogonal distance regression method was of similar magnitude to that obtained by activated carbon (158.5 mg g^{-1}) but cork bark (29.9 mg g^{-1}) resulted to be about five times less effective than activated carbon. The textural results indicate that grape stalks and cork bark present a remarkable macropore surface area with a minor contribution of mesopores. The large pore size exhibited by both sorbents surface seems to be unable to efficiently uptake such small basic fuchsin molecules. The lower sorption capacity shown by cork bark compared to that of grape stalks may be explained by surface chemistry effects. Basic fuchsin sorption is not favoured by the presence of acidic functional groups on the sorbent surface. Acidic groups such as hydroxyl groups may promote the formation of hydration clusters that effectively reduce and/or hinder electrostatic and π interactions between basic fuchsin and the sorbents surface. FTIR analysis revealed that lignin moieties on the sorbents surface play a significant role on the dye sorption. As a final remark, the knowledge of some physical and chemical properties of the sorbents can be helpful for predicting their sorption affinity for organic pollutants.

Keywords: Basic fuchsin; Cork bark; Grape stalks; Activated carbon; FTIR; Lignin moieties; π interactions; Orthogonal distance regression method

*Corresponding author.

1. Introduction

Textile, printing and food industries among others use dyes to colour their products and, as a result, a considerable amount of coloured wastewater is generated. The resulting wastewater is difficult to treat using conventional wastewater treatment methods since dyes are very stable to light and oxidizing agents, and are resistant to aerobic digestion [1]. Basic violet 14 also denominated basic fuchsin (BF) is soluble in water and alcohol, and is widely employed in colouring textiles and leathers. BF is also used to stain collagen, muscle, or mitochondria [2]. It possesses anaesthetic, bactericidal (gram positive) and fungicidal properties [3]. The physical contact with the dye may cause gastrointestinal irritation with nausea, vomiting, while the inhalation of the dye may cause irritation to the respiratory tract and several damage to organs such as blood, liver, spleen and thyroid [4,5]. Toxicity of this dye has been reported to cause carcinogenesis and mutagenesis in humans and animals [6,7].

Globalization and scarcity of water require from the companies high concern for wastewater treatment and water recycling [8]. Adsorption on activated carbon is established to be a very efficient treatment to remove dyes from wastewater but the high regeneration costs of this treatment encourage researchers to find out alternatives such as low-cost adsorbents. A large number of waste materials from agriculture and food-industries have been tested for dye removal from aqueous solutions [9–13]. Nevertheless, removal of BF [10,14–16] and in general basic dyes [17,18] by biosorbents has been scarcely investigated in the recent past.

For the last few years, our group has focused its research on using low-cost sorbents based on vegetable wastes for the removal of organic compounds [19–21]. In this work, grape stalks (GS) and cork bark (CB), vegetables that are abundant after wine production and wine corks manufacturing, respectively, have been investigated for the removal of BF.

With the aim to elucidate the factors influencing the sorption process, physico-chemical characteristics of both sorbents have been determined. The physico-chemical characterization included Boehm titration (acidic groups), elemental analysis, Fourier transform infrared rays (FTIR) and mercury porosimetry (surface area and pore size distribution). The parameters obtained from physical and chemical characterization of the sorbents resulted to be a useful tool to discuss the sorption behaviour of the studied sorbents.

2. Experimental

2.1. Materials

GS and CB wastes were kindly supplied by two industries from Girona region dealing with wine production and tap manufacturing, respectively. Activated carbon (AC) was supplied by Panreac (Granulated n.3 QP). GS waste was previously rinsed with abundant distilled water to remove dirty particles and colour, and then dried in an oven at 100°C. Rinsing was not needed in the case of CB waste. Both GS and CB wastes were ground in a coffee grinder (Taurus MS 50) and then sieved (Screener FT-91) for a particle size between 0.63 and 0.75 mm. Activated carbon was also sieved to get the same range of particle size.

A 1,000 mg L⁻¹ of basic violet 14 stock solution, commonly named BF, was prepared by solving the appropriate amount of the dye in deionized water (Millipore Direct Q4 Water Purification system). This solution was used to prepare the required initial concentrations to carry out sorption experiments. The structural formula and chemical characteristics of BF are shown in Fig. 1. For pH adjustment, 0.1 M solutions of NaOH and HCl were used. Initial and final pH was recorded with a pH meter (Crison GLP-21). All reagents were of analytical grade and purchased from Panreac, Barcelona, Spain.

2.2. Methods

2.2.1. Physical characterization

Pascal 140 and Pascal 240 porosimeters were used to investigate GS and CB macroporous and meso/microporous structure, respectively. Pascal 140 investigation range lies between 0.1 and 400 kPa (vacuum-4 atm). Pascal 240 range lies between 0.1 and 20 MPa (2–20 atm). These instruments provided data about

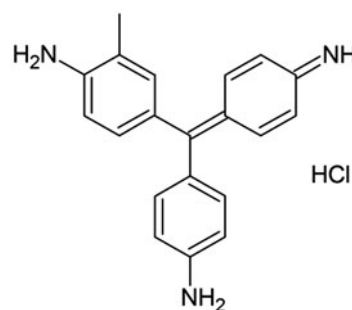


Fig. 1. Basic violet 14 (BF) chemical structure (C₂₀H₁₉N₃HCl, MW: 337.85 g mol⁻¹, S: 4 g L⁻¹).

pore size/volume distribution, particle size distribution, bulk density and specific surface of GS and CB.

2.2.2. Chemical characterization

The elemental analyses (C, H, N and S) of GS and CB were determined using an Elemental Analyzer CE instrument EA1110. Limits of detection were 1.2% for N, 0.72% for C, 0.2% for H and 0.44% for S. Oxygen content was calculated by a difference that takes into account all the mineral content.

Acidic properties of GS and CB surfaces were determined by titration following the Boehm's method [22]; 1 g of cork biomass was placed into an Erlenmeyer flask containing 0.1 L of 0.1 M NaHCO₃, Na₂CO₃ or NaOH and placed into a thermostated shaker for 48 h. Strongly acidic carboxylic groups are neutralized by NaHCO₃; weak acidic groups (i.e. carboxylic, lactonic and enolic) are neutralized by Na₂CO₃; NaOH consumes all those groups. Thus, the difference between NaOH and Na₂CO₃ consumption corresponds to the weakly acidic phenolic groups.

2.2.3. Sorption studies of BF

Batch equilibrium experiments were conducted at room temperature (20 ± 2°C) on a rotary shaker (rotator STR4, Stuart Scientific Bibby) at 30 rpm, using 25 mL glass tapered tubs. In all experiments, 0.1 g of the GS, CB and AC sorbents (particle size 0.63–0.75 mm) was put into contact with constant agitation with 15 mL of dye solutions. When sorption equilibrium was achieved, sorbent was separated from the liquid by centrifugation (Jouan C R312) at 4,000 rpm for 10 min; the pH was recorded (Crison GLP 21); and the filtrates were analysed for dye concentration by spectrophotometry (Shimadzu UV-160) at λ_{max} at 550 nm.

Control experiments were conducted under the same experimental conditions using deionized water without sorbate. The following equation was used to compute the specific uptake by the sorbent:

$$q = (C_i - C_f) \cdot V/w \quad (1)$$

where C_i and C_f are the initial and final dye concentration; V (in L) is the solution volume; and w (in g) is the amount of dry sorbent used.

When studying the effect of pH, solution initial pH was varied within the range 1–10, BF initial concentration was 100 mg L⁻¹ and the agitation time was 90 min.

For sorption kinetics experiments, the initial dye concentration was 100 mg L⁻¹, and the pH was 6.0. Dye solutions of different initial concentrations (50–1,000 mg L⁻¹) were used to obtain sorption isotherms at 20 ± 2°C. All experiments were performed in duplicate and the average results are presented.

2.2.4. FTIR analysis

With the aim to elucidate the functional groups on the sorbents surface involved in BF sorption, FTIR analysis of BF and CB before and after BF sorption was carried out. Spectra were obtained using KBr pellets and were recorded on a Galaxy 5,000 FTIR spectrometer (Mattson Instrument Co., Madison, WI). To prepare the pellets, about 2 mg of the sample was ground for 1 to 2 min together with about 200 mg of KBr (FT-IR grade, Acros Organics). All FTIR spectra were measured in the 3,500 to 400 cm⁻¹ range by co-addition of 32 scans with a resolution of 2 cm⁻¹.

3. Results

3.1. Physical characterization

Table 1 gives the specific surface area (S_e), bulk density, total cumulative pore volume (V_c), average pore diameter (D_p) and % porosity of GS and CB. As seen in this table, the surface area of CB is two times higher than that of GS. The larger surface area of CB compared to that of GS is mainly due to the presence of a larger number of porous. This explanation is supported by the higher cumulative volume, porosity percentages and the lower density presented by CB sorbent. As seen in Table 1, the average pore diameter was higher in GS (43.20 μm) than in CB (2.68 μm).

According to pore sizes, nanoporous materials are classified into microporous materials (pore width < 2 nm), mesoporous materials (pore width between 2 and 50 nm) and macroporous materials (pore width > 50 nm). Fig. 2 shows the pore size distribution of GS and CB. Both samples porosity is

Table 1
Specific surface area (S_e), bulk density and pore size distribution (total cumulative pore volume (V_c), average pore diameter (D_p) and % porosity) of (GS) and (CB)

	S_e (m ² /g)	Bulk density (g/cm ³)	V_c (mm ³ /g)	D_p (μm)	% porosity
GS	21.60	0.90	495.57	43.20	45.06
CB	52.14	0.15	6039.50	2.68	91.40

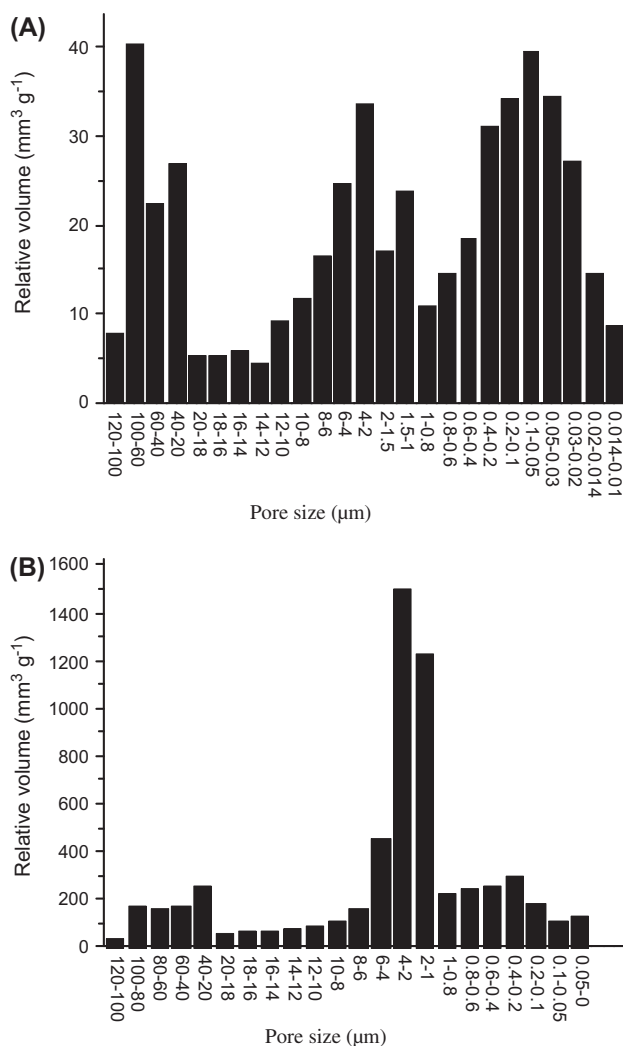


Fig. 2. Pore size distribution of GS (A) and CB (B).

primarily contributed by macropores with a different profile of pore size distribution. GS shows a broad macropore distribution over a wide range of pore widths with three maximum peaks of relative volume ranging from 31–40 mm³ g⁻¹. In contrast, CB clearly shows two maximum peaks of relative volume at 1,503 and 1,227 mm³ g⁻¹ which correspond to the pore width range 4–2 μm and 2–1 μm, respectively. Macropores contribution of CB in the pore width range between 20 and 40 μm is mainly due to the structure of cork itself which is partially composed of hollow cells of macropore size [23]. The specific volume of these hollow cells with respect to the total volume represents 4% of the total porosity. It is important to remark that these cells are inaccessible to aqueous pollutants because they internally contain a large quantity of gas, presumably similar to air [24].

Minor contribution of mesopores and less micropores was observed in both sorbents. The data provided by the porosity analysis indicate that pore sizes between 0 and 50 nm covers a specific surface of 25.97 and 14.30 m² g⁻¹ of CB and GS, respectively. A maximum peak of pore radius in the range 0.05–0.025 μm and 0.2–0.1 μm was found for GS and CB, respectively (Fig. 2).

3.2. Chemical characterization

Table 2 presents the elemental analysis, polarity index (i.e. (O + N)/C) and the acidic functional groups determined by Boehm titration. In the same table, the value of the point of zero charge (pH_{pzc}) determined in a previous work [25] is shown. Elemental analysis shows that GS and CB elemental percentages are within the range of values reported for typical agricultural residues (%C ranges from 41.23 to 53%; %H from 4.63 to 6.58% and %N from 0.7 to 2.63%) [26].

The polarity coefficient (O + N)/C is an important parameter inversely correlated with the aromatic character of the sample. The polarity coefficients found for GS and CB are significantly different (i.e. 0.83 and 0.42, respectively), while GS polarity index is in the range of those of cellulose and chitin (0.84–1.94) and CB polarity index in the range of some commercial lignins (0.33–0.65) [27]. The more aliphatic character of CB compared to GS is confirmed by the higher hydrogen content and is presumably due to the high presence of suberin (40–60%) in its composition [28]. Suberin is a polymeric material of aliphatic character with ester and phenolic functionalities. This biopolymer is almost not present in GS.

The values of CB and GS polarity indexes could be a good indicative of the sorption affinities presented by these two sorbents. It was reported by several authors that this coefficient is inversely correlated with the hydrophobic pollutants sorption [29,30]. Taking into account this correlation, GS should have more sorption affinity for hydrophilic pollutants and CB for hydrophobic pollutants.

As seen in Table 2, CB presents a higher number of acidic groups than GS. The higher acidic nature of CB compared to GS is consistent with the pH_{pzc} values reported in our previous work for CB (pH_{pzc} 3.6) and for GS (pH_{pzc} 5.0) [25]. The higher content of phenolic groups of CB is probably due to the higher content of lignin (17–30%) of this sorbent [28] compared to the lignin content values found for GS (6.5%) (unpublished data).

Table 2

Elemental analysis, point of zero charge (pH_{pzc}) and acidic functional groups of (GS) and (CB). TAG stands for total acidic groups, SAG for strong acidic groups, PG for phenolic groups and WAG for weak acidic groups

	%C	%H	%N	%S	%O ^a	(O+N)/C	pH_{pzc} ^b	TAG (mmol g^{-1})	SAG	PG	WAG
GS	42.4	5.5	0.8	n.d.	46.3	0.83	5.0	1.35	0.447	0.775	0.143
CB	58.4	7.9	0.4	n.d.	32.3	0.42	3.6	1.88	0.733	0.915	0.232

^aCorrected by mineral content.

^bFiol and Villaescusa [25].

3.3. Sorption studies

3.3.1. Effect of pH

The spectra of 100 mg L^{-1} BF solutions adjusted at different pH values within the range 1.0–9.8 are shown in Fig. 3. As seen, BF color intensity and therefore visible light absorption depend on the solution pH. For instance, at wavelength of 550 nm, commonly used in BF absorbance measurements, the absorbance is high (0.7 units) at pH between 3 and 6, decreases significantly at extreme pH (0.1 units at pH 1.7 and 9.8), and is almost null at pH 1.0. The differences in light absorbance must be attributed to the effect of pH on BF surface charge and ionization.

BF removal by GS, CB and AC was investigated in the pH range 1.0–10.0. Taking into account the effect of pH on BF light absorbance, BF concentration was determined at $\lambda = 550 \text{ nm}$ by using a specific calibration curve for each of the tested solution pH. It must be remarked that in most of the papers dealing with BF sorption, the authors do not mention at which pH they obtained the calibration curve when studying the effect of pH on the dye sorption [14,16,31]. The percentage of BF removed by the three sorbents investigated in this study as a function of pH is plotted in Fig. 4. As seen in the figure, BF sorption onto AC, GS and CB was maximum and insignificantly affected by

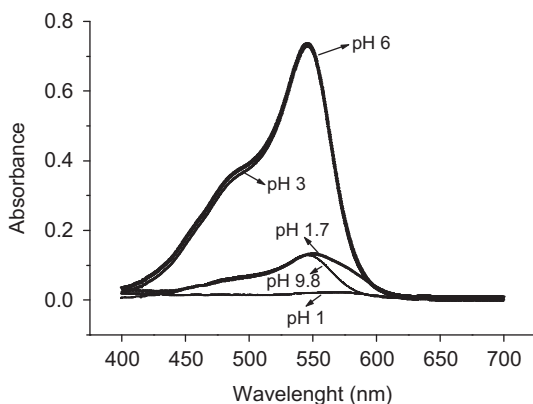


Fig. 3. Spectra of (BF) at different pH values. BF concentration: 100 mg L^{-1} .

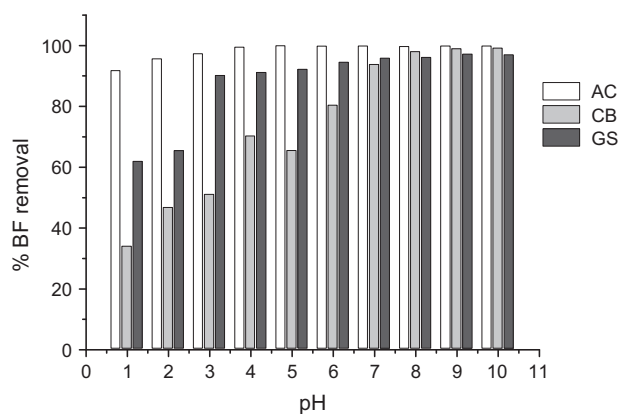


Fig. 4. Percentage of (BF) removal by (GS), (CB) and activated carbon (AC) as a function of solution initial pH. BF initial concentration = 100 mg L^{-1} , agitation time 90 min.

pH within the pH ranges 4–10, 3–10 and 7–10, respectively. To understand the sorption mechanism at the different pH values, it is necessary to take into account that pH of the solution also affects the surface charge of the sorbents. This point will be discussed in Section 4. Taking into account the results shown in Fig. 4, pH 6.0 was selected to carry out kinetics and equilibrium experiments because at this pH the three sorbents showed high sorption yields and null or slight pH adjustment of the 100 mg L^{-1} BF solution was required.

Previous studies also reported the sorption pH-dependence of BF sorption. BF maximum sorption on deoiled soya and bottom ash was within the pH range 8.0–10.0 [31] and was at pH 7.0 on a living biomass (*Hydrillaverticillata*) [16]; Bhole et al. [14] reported that BF sorption on fungal biomass was independent of pH within the pH range 5.0–7.0. The different optimum pH values found for BF sorption put into evidence the important role of the sorbent surface chemistry on the sorption process.

3.3.2. Sorption kinetics and equilibrium studies

Sorption kinetics profiles of BF sorption obtained at $20 \pm 2^\circ \text{C}$ are shown in Fig. 5. Data were submitted

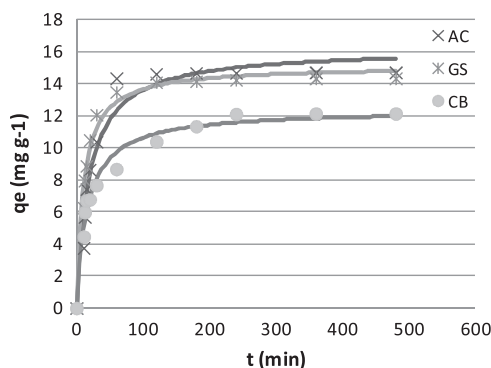


Fig. 5. Basic fuchsin (BF) sorption onto activated carbon (AC) (GS) and (CB) as a function of time. BF initial concentration 100 mg L^{-1} , sorbent concentration 6.66 g L^{-1} , pH 6.0. Symbols are the experimental data, solid lines represent predicted data by pseudo-second model.

to the pseudo-second-order kinetics model [32] given by the equation:

$$\frac{dq}{dt} = K_2(q_e - q_t)^2 \quad (2)$$

where q_e and q represent the amount of dye adsorbed (mg g^{-1}) at equilibrium and at any time t , respectively, and K_2 represents the sorption rate constant (L min^{-1}). The analytical solution for Eq. (2) at the initial concentration $t = 0$, $q_t = 0$, is given by:

$$q_t = \frac{q_e^2 K_2 t}{1 + q_e K_2 t} \quad (3)$$

q_e and K_2 can be obtained by non-linear regression by minimizing the sum of square errors (SSR):

$$SSR = \sum_{i=1}^{i=N} (q_{\text{exp}} - q_t)^2 \quad (4)$$

The initial sorption rate (h) was calculated as follows:

$$h = K_2 q_e^2 \quad (5)$$

The calculated kinetic parameters presented in Table 3 show that BF sorption by the studied sorbents is quite fast: 50% of dye removal takes place in 15 min in the case of AC and GS and in 20 min in case of CB. The equilibrium was achieved within 240 min for AC and 480 min for both GS and CB. GS shows a higher initial sorption rate compared to AC but the former exhibits a lower amount of dye sorbed at equilibrium. CB shows the lowest sorption initial rate and the lowest sorption at equilibrium time. The SSR values together with the correlation coefficients closer to the unity (0.970 for AC, 0.981 for GS and 0.979 for CB) confirm that for all the studied systems the sorption process follows a pseudo-second-order mechanism. The assumption behind the pseudo-second-order model is due to chemisorption that may occur by the polar functional groups of lignin and/or cellulose [32]. The functional groups and the mechanisms involved are discussed in Section 4.

Kinetics of BF sorption was also studied at $15 \text{ }^\circ\text{C}$ and $30 \text{ }^\circ\text{C}$ (results not shown). It was observed that temperature change has almost no effect on BF sorption onto the studied sorbents; therefore, a thermodynamic study of BF sorption was not undertaken. Similar observation about the effect of temperature was reported by Wang and Lin [33].

3.3.3. Sorption isotherms

Equilibrium sorption data shown in Fig. 5 were fitted to the Langmuir-type adsorption isotherm model,

$$q = \frac{q_{\text{max}} b C_{\text{eq}}}{1 + b C_{\text{eq}}} \quad (6)$$

where q is the sorbed amount (mg g^{-1}), q_{max} is the maximum sorbate uptake (mg g^{-1}), C_{eq} is the equilibrium concentration of sorbate in solution after

Table 3

Pseudo-second order rate constants and Langmuir parameters for (BF) sorption onto activated carbon (AC), (GS) and (CB). Sorption kinetics (initial BF concentration 100 mg L^{-1} , sorbent concentration 6.66 g L^{-1} , pH 6.0). Isotherm (temperature $20 \pm 2 \text{ }^\circ\text{C}$, sorbent concentration 6.66 g L^{-1} , agitation time 90 min, pH 6.0)

BF Sorbent	Sorption kinetics				Sorption isotherm		
	K_2 ($\text{g mg}^{-1} \text{ min}^{-1}$)	q_e (mg g^{-1})	h mg (g min)^{-1}	SSR	q_{max} (mg g^{-1})	b	SSR_{ODR}
AC	0.00321	16.20	0.84	11.62	158.54	0.88	4.77×10^{-4}
GS	0.00622	15.11	1.42	4.11	106.79	0.018	4.65×10^{-3}
CB	0.00489	12.38	0.75	3.14	29.91	0.013	1.53×10^{-2}

adsorption (mg L^{-1}), and b is the equilibrium constant related to the energy of sorption which quantitatively reflects the affinity between the sorbent and sorbate.

The Langmuir isotherm parameters, q_{max} and b , were obtained using the orthogonal distance regression (ODR) method. Recently, Poch and Villaescusa [34] reported that the ODR method gives the most accurate estimates of the isotherm parameters among the different regression methods when C_{eq} and C_0 are known with some experimental error. The ODR method relies on minimizing the sum of square relative errors with regard to both C_{eq} and q (Eq. 5). Regression computations were carried out using Matlab R2008b. Specifically, the optimization was performed by applying the Generalized Reduced Gradient method, and the library GRG2 [35] was employed.

$$SSR_{\text{ODR}} = \sum_{i=1}^N \left(\frac{C_{\text{eq},i,\text{exp}} - C_{\text{eq},i,\text{calc}}}{C_{\text{eq},i,\text{exp}}} \right)^2 + \left(\frac{q_{i,\text{exp}} - q_{i,\text{calc}}}{q_{i,\text{exp}}} \right)^2 \quad (7)$$

The obtained results for q_{max} and b for BF sorption onto the three studied sorbents estimated by ODR method as well as the corresponding SSR values are presented in Table 3. From the estimated model parameters, the calculated curves were superimposed to the experimental values in Fig. 6.

As shown in Table 3, GS shows similar BF sorption capacity (106.79 mg g^{-1}) than AC (158.54 mg g^{-1}) and CB capacity for BF (29.91 mg g^{-1}) is five times lower than that of AC. The second Langmuir constant, b , is the measure of BF sorption energy which reflects the affinity of the tested materials for BF sorption. As seen

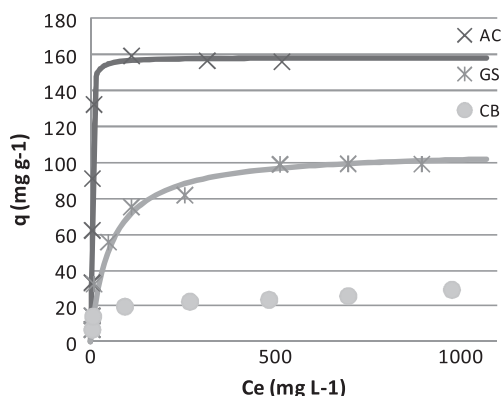


Fig. 6. Sorption isotherms of (BF) sorption onto activated carbon (AC), (GS) and (CB). Solid lines represent predicted data by the Langmuir model, and the symbols are the experimental data. Temperature $20 \pm 2^\circ\text{C}$, sorbent concentration 6.66 g L^{-1} , pH 6.0, contact time 240 min (AC), 480 min (GS and CB).

in Table 3, activated carbon shows the highest affinity (0.88 L mg^{-1}) as compared to GS (0.018 L mg^{-1}) and CB (0.013 L mg^{-1}).

When comparing GS sorption capacity for BF with the reported in literature for other low-cost sorbent materials, GS capacity for BF was similar to those found by Jiang et al. [36] using bentonite (147.49 and 100 mg g^{-1}) and much higher than those found by Saranya et al. [16] (22.2 mg g^{-1}) using *Hydrilla verticillata* and Gupta et al. [31] (9.1 and 10.9 mg g^{-1}) using bottom ash and deoiled soya.

3.4. FTIR analysis

Fig. 7 shows both raw and BF loaded spectra of GS and CB. The spectra indicate that lignin plays a significant role on BF sorption onto both sorbents. This is confirmed by the shift of two characteristic bands associated to the lignin structure: the band associated to the aromatic ring vibrations (i.e. C=C bonds) and the band associated to the C–O stretching of the methoxy group ($-\text{OCH}_3$) of the aromatic ring. In the case of CB, the increase in wave number of aromatic C=C band from 1512.9 cm^{-1} to 1516.7 cm^{-1} could reflect π – π interactions between π aromatic rings donors of BF and π acceptor groups in the sorbent (i.e. aromatic rings of lignin) [37]. Other bands related to the aromatic vibrations (i.e. $1,598 \text{ cm}^{-1}$) were overlapped with the characteristic bands of BF. Concerning the bands attributed to C–O stretching (corresponding to the methoxy group of lignin), a shift in the band from $1,035 \text{ cm}^{-1}$ to $1,031.8 \text{ cm}^{-1}$ for GS and to $1,033.2 \text{ cm}^{-1}$ for CB was observed. Nevertheless, it must be remarked that these bands can be also attributed to C–O bonds of cellulose/hemicelluloses constituents [38].

The band associated to the C–H bonds shifted from $1,444.4 \text{ cm}^{-1}$ to $1,439 \text{ cm}^{-1}$. This shift could reflect H– π interactions between aromatic rings from BF and methyl groups from lignin ($-\text{OCH}_3$) [37]. The bands at about $1,598 \text{ cm}^{-1}$, $1,554 \text{ cm}^{-1}$, $1,336 \text{ cm}^{-1}$, $1,283 \text{ cm}^{-1}$ and $1,155 \text{ cm}^{-1}$ are characteristic of the BF spectrum.

4. Discussion

Physical and chemical properties have been determined for both GS and CB sorbents. The porosity results showed that CB in spite of having a higher macro and mesoporous surface than GS (Table 1) shows a lower sorption capacity for BF (Table 3). This could be due to the fact that the pore size is too big (several μm) (Table 1) to confine such small-sized BF molecules ($1.06 \times 1.05 \times 0.48 \text{ nm}$) [39]. An improvement

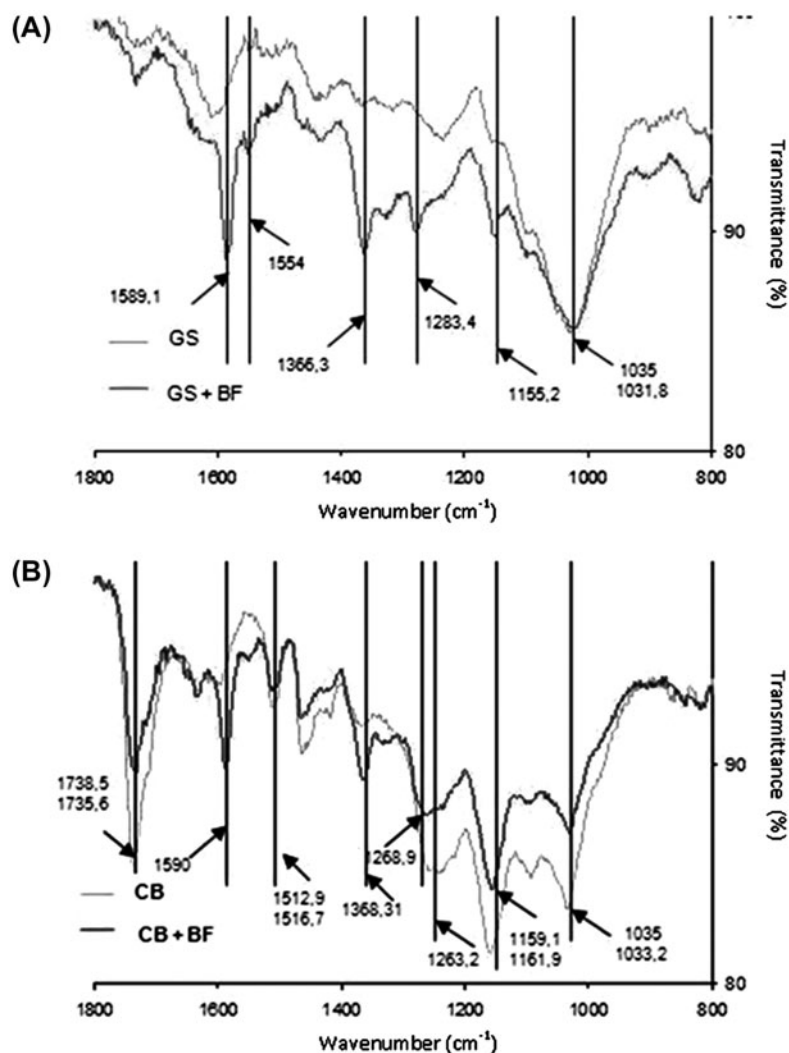


Fig. 7. FTIR spectra of (A) (GS) and GS loaded with (BF), (B) (CB) and CB loaded with BF. The upper and lower wavenumbers correspond to the top and bottom spectra, respectively.

of the physical bonding between the studied sorbents and BF could be achieved by the production of activated carbon from these two wastes; thereby, increasing the micropore surface area [26].

The most important contribution of the chemical BF sorption onto GS and CB over the physical is reflected by the polarity index. As mentioned before, GS exhibits a high polar character (i.e. $(O + N)/C = 0.83$) which is in good accordance with the higher sorption affinity for BF, compound with hydrophilic character (solubility in water 4 g L^{-1}). This confirms that polarity index is a key sorption indicator to predict the affinity of sorbents for organic compounds.

At the pH value used in this work (pH 6.0), the sorbents surface is negatively charged ($\text{pH} > \text{pH}_{\text{pzc}}$) mainly due to the deprotonation of both weak acids (i.e. carboxylic, lactonic and phenolic) and strong

acidic groups (i.e. carboxylic groups) (pK_a between 3 and 6), while phenolic groups (pK_a about 9.5–10.5) are not expected to give a deprotonation. On the other hand, BF exists mainly as cationic species all over the pH range 2–10.

In principle, it would be expected that the more negatively charged surface of CB than that of GS would favour electrostatic interactions with the positively charged BF ions [40]. However, CB was found to be less effective than GS. These unexpected results could be due to the higher presence of acidic groups in CB (Table 2) that may unfavour the interactions between BF and the groups on the sorbent surface. The preferential H-bonding of water to some oxygen functional groups (i.e. carboxylic and phenolic groups) can create water clusters around them, thus reducing and/or hindering interactions between BF

and the sorbent. This idea of competition between organic compounds and water molecules for the surface acidic groups was reported by Radovic et al. [41]. These authors used an as-received activated carbon and the oxidized form of this carbon and they found that the oxidized form possessed less sorption capacity. The authors justified the decrease of sorption because of the strong preference of water for forming hydrogen bonds with the acidic groups on the sorbent surface.

As suggested by the FTIR spectra, lignin moieties play a significant role on BF sorption. As mentioned above, CB has more lignin content than GS and therefore higher alcoholic groups content. These alcoholic groups that are protonated at pH 6.0 could be more efficient in clustering water molecules, thus preventing the access of BF molecules to the sorbent surface (i.e. lignin moieties and extractives) with consequent decrease of BF sorption capacity.

Moreover, lignin of CB is located on the secondary cell wall, thus it is more accessible to organic pollutants [23], and the hydroxyl groups contained in the lignin moieties are consequently more accessible to water molecules. The preferential formation of H-bonds between water molecules and surface oxygen groups was previously reported for the sorption of phenol–water mixture [42].

In summary, the main interactions that could occur between both sorbents and BF could be: (1) π – π interactions between aromatic cores of BF and sorbent surface aromatic groups; (2) electrostatic interactions between the sorbent negatively charged mainly from carboxylic groups and N^+ groups of BF; (3) cation– π interactions: the N^+ centres were found to make favourable interactions with the π -electron cloud of aromatic side chains [43]; and 4) H– π interactions between the π aromatic system of BF and –OH and –COOH groups [44]. Liao et al. [45] investigated the contribution of different interactions in a system formed by nitrogen heterocyclic compounds (i.e. pyridine, indole and quinoline) and a carbonaceous material. They found that the dominating interactions were physical (45% contribution) followed by hydrophobic and electrostatic interactions whereas π – π interactions had only 8% contribution.

Recently, Cotoruelo et al. [15] reported that the forces involved in the sorption of BF by activated carbon prepared from lignin are low, like Van der Waals types.

5. Conclusions

This research work was focused on the investigation of potential ability of GS and CB for the removal

of BF. As a general conclusion, it may be stated that GS is an efficient biosorbent for the removal of BF and, given that it is a low-cost biosorbent, may be considered as a viable alternative to activated carbon.

The following specific conclusions arise from this work:

- Langmuir parameters estimated by ODR method showed that maximum sorption capacity of activated carbon and GS was of similar order of magnitude (i.e. 158.5 mg g^{-1} for activated carbon and 106.8 mg g^{-1} for GS) and CB showed the lowest sorption capacity (29.9 mg g^{-1}).
- Physico-chemical characterization was useful to explain the different sorption behaviour of GS and CB towards BF.
 - (a) Both sorbents are dominated by a macroporous structure. The pores of GS and CB are too large to confine such small BF molecules.
 - (b) The polarity index which is easily determined from the sorbents elemental analysis is a very useful parameter to predict the sorbents sorption behaviour towards organic pollutants. The higher polar character of GS determines its greater capacity for BF sorption.
 - (c) The lower surface acidity of GS is thought to be mainly responsible for its higher sorption capacity for BF. The strong affinity of hydroxyl groups in cork bark lignin moieties to create water clusters may reduce and/or hinder electrostatic and π interactions between cork bark and the dye.
 - (d) FTIR spectra confirm that lignin moieties play a significant role on BF sorption.

The final remark is a recommendation for future sorption studies of organic pollutants.

Before performing sorption experiments, it is advisable to determine a set of physical and chemical sorbent parameters which are found to be useful to predict the binding affinities of sorbents for organic compounds.

Acknowledgements

Thanks are due to Gloria Bolivar for her help in the experimental work and to Dr S. Sammartano and Dr C. de Stefano from the Dipartimento de Chimica Inorganica, Chimica Analitica e Chimica Fisica of the Università degli studi di Messina for performing the porosimetry analysis. This work has been financially supported by Ministerio de Ciencia e Innovación,

Spain, Projects CTM 2008-06776-C02-01 and CTM 2010-15185.

References

- [1] V.J.P. Poots, G. McKay, J.J. Healy, The removal of acid dye from effluent using natural adsorbents-II *Water Res.* 10 (1976) 1067–1070.
- [2] L. Luna, *Manual of Histologic Staining Methods of the AFIP*. 3rd ed., McGraw-Hill, New York, NY, 1968.
- [3] F.L. Carson, *Histotechnology: A self-instructional text*. 2nd ed., American Society clinical Pathology, Chicago, 1997.
- [4] A. Crandall, E. Oldberg, A.C. Ivy, Contributions to the physiology of the pancreas: The elimination of dyes in the external secretion of the pancreas. *Am. J. Physiol.* 89 (1929) 223–229.
- [5] S.C. Rogers, D. Burrows, D. Neill, Percutaneous absorption of phenol and methyl alcohol in magenta paint B.P.C, *British J. Dermatol.* 98 (1978) 559–560.
- [6] N.A. Littlefield, B.N. Blackwell, C.C. Hewitt, D.W. Gaylor, Chronic toxicity and carcinogenicity studies of gentian violet in mice, *Toxicol. Sci.* 5 (1985) 902–912.
- [7] P.P. Puglisi, Antimutagenic activity of actinomycin D and basic fuchsin in *Saccharomyces Cerevisiae*, *Mol. Gen. Genet.* 103 (1968) 248–252.
- [8] B.C. Bates, Z.W. Kundzewicz, S. Wu, J.P. Palutikof, Climate change and water. Technical Paper IV, Intergovernmental Panel on Climate Change, IPCC Secretariat, Geneva, 210 p, 2008.
- [9] V.K. Garg, M. Amita, R. Kumar, R. Gupta, Basic dye (methylene blue) removal from simulated wastewater by adsorption sawdust: A timber using Indian Rosewood industry waste, *Dyes Pigm.* 63 (2004) 243–250.
- [10] V.K. Gupta, Application of low-cost adsorbents for dye removal—A review, *J. Environ. Manage* 90 (2009) 2313–2342.
- [11] D. Kavitha, C. Namasivayam, Recycling coir pith, an agricultural solid waste, for the removal of procion orange from wastewater, *Dyes Pigm.* 74 (2007) 237–248.
- [12] H. Lata, V.K. Garg, R.K. Gupta, Removal of a basic dye from aqueous solution by adsorption using *Parthenium hysterophorus*: An agricultural waste, *Dyes Pigm.* 74 (2007) 653–658.
- [13] P. Sharma, H. Kaur, M. Sharma, V. Sahore, A review on applicability of naturally available adsorbents for the removal of hazardous dyes from aqueous waste, *Environ. Monit. Assess.* 183 (2011) 151–195.
- [14] B.D. Bhole, B. Ganguly, A. Madhuram, D. Deshpande, J. Joshi, Biosorption of methyl violet, basic fuchsin and their mixture using dead fungal biomass, *Curr. Sci.* 86 (2004) 1641–1645.
- [15] L.M. Cotoruelo, M.D. Marqués, J. Rodríguez-Mirasol, J.J. Rodríguez, T. Cordero, Cationic dyes removal by multilayer adsorption on activated carbons from lignin, *J. Porous. Mater* 18 (2011) 693–702.
- [16] G. Saranya, P. Saravanan, K. Dharmendira, S. Renganathan, Equilibrium uptake and bioaccumulation of basic Violet 14 using submerged macrophyte *Hydrilla verticillata*, *CLEAN - Soil Air Water* 39 (2011) 283–288.
- [17] J. Kalpana, P. Saravanan, N. Nagendra Gandhi, S. Renganathan, Equilibrium modelling on biosorption of basic violet 1 dye using *Calotropis gigantea* biomass, *Indian J. Environ. Prot.* 31 (2011) 825–832.
- [18] S. Pankaj, K. Harleen, S. Monika, M. Sharma, V. Sahore, A review on applicability of naturally available adsorbents for the removal of hazardous dyes from aqueous waste, *Environ. Monit. Assess.* 183 (2011) 151–195.
- [19] M.À. Olivella, P. Jové, A. Oliveras, The use of cork waste as a biosorbent for persistent organic pollutants—Study of adsorption/desorption of polycyclic aromatic hydrocarbons, *J. Environ. Sci. Health., Part A* 46 (2011) 1–9.
- [20] M.À. Olivella, N. Fiol, F. de la Torre, J. Poch, I. Villaescusa, A mechanistic approach to methylene blue sorption on two vegetable wastes: Cork bark and grape stalks, *Bioresources* 7 (3) (2012) 3340–3354.
- [21] I. Villaescusa, N. Fiol, J. Poch, A. Bianchi, C. Bazzicalupi, Mechanism of paracetamol removal by vegetable wastes: The contribution of π - π interactions, hydrogen bonding and hydrophobic effect, *Desalination* 270 (2011) 135–142.
- [22] T.S. Psareva, O.I. Zakutevskyy, N.I. Chubar, V.V. Strelko, T.O. Shaposhnikova, J.R. Carvalho, M. Joana Neiva Correia, Uranium sorption on cork biomass, *Colloids Surf., A: Physicochem. Eng. Aspects*, 252 (2005) 231–236
- [23] H. Pereira, Cork: Biology, production and uses. in: H. Pereira (Ed.), *The Chemical Composition of Cork*, 2007, Amsterdam, Elsevier, pp. 55–101.
- [24] M.E. Rosa, H. Pereira, The effect of long-term treatment at 100°C–150°C on structure, chemical-composition and compression behaviour of cork, *Holzforschung* 48 (1994) 226–232.
- [25] N. Fiol, I. Villaescusa, Determination of sorbent point zero charge: Usefulness in sorption studies, *Environ. Chem. Lett.* 7 (2009) 79–84.
- [26] O. Ioannidou, A. Zabaniotou, Agricultural residues as precursors for activated carbon production—A review, *Renew. Sust. Energ. Rev.* 11 (2007) 1966–2005.
- [27] X. Wang, R. Cook, S. Tao, B.S. Xing, Sorption of organic contaminants by biopolymers: Role of polarity, structure and domain spatial arrangement, *Chemosphere* 66 (2007) 1476–1484.
- [28] P. Jové, M.À. Olivella, L. Cano, Study of the variability in chemical composition of bark layers of *Quercus suber* L. from different production areas, *Bioresources* 6 (2) (2011) 1806–1815.
- [29] D.W. Rutherford, C.T. Chiou, D.E. Kile, Influence of soil organic matter composition on the partition of organic compounds, *Environ. Sci. Technol.* 26 (1992) 336–340.
- [30] B. Xing, W.B. McGill, M.J. Dudas, Cross-correlation of polarity curves to predict partition coefficients of non-ionic organic contaminants, *Environ. Sci. Technol* 28 (1994) 1929–1933.
- [31] V.K. Gupta, A. Mittal, V. Gajbe, J. Mittal, Adsorption of basic fuchsin using waste materials-bottom ash and deoiled soya- as adsorbent, *J. Colloid. Interf. Sci.* 319 (2008) 30–39.
- [32] Y.S. Ho, Removal of copper ions from aqueous solution by tree fern, *Water Res.* 37 (2003) 2323–2330.

- [33] X.S. Wang, H.Q. Lin, Adsorption of basic dyes by dried waste sludge: Kinetic, equilibrium and desorption studies, *Desalin. Water Treat.* 29 (2011) 10–19.
- [34] J. Poch, I. Villaescusa, Orthogonal distance regression: A good alternative to least squares for modelling sorption data, *J. Chem. Eng. Data* 57 (2012) 490–499.
- [35] L.S. Lasdon, A.D. Warren, Generalized reduced gradient software for linearly and nonlinearly constrained problems, in: H.J. Alphen aa del Rijn (Ed.), *Design and Implementation Optimization Software*, The Netherlands, 1979, pp. 363–396.
- [36] Y.X. Jiang, H.J. Xu, D.W. Liang, Z.F. Tong, Adsorption of Basic Violet 14 from aqueous solution on bentonite, *C.R. Chimie*, 11 (2008) 125–129.
- [37] M. Keiluweit, M. Kleber, Molecular-level interactions in soils and sediments: The role of aromatic-systems, *Environ. Sci. Technol.* 43 (2009) 3421–3429.
- [38] M. Haussard, I. Gaballah, N. Kanari, Ph de Donato, O. Barrès, F. Villieras, Separation of hydrocarbons and lipid from water using treated bark, *Water Res.* 37 (2003) 362–374.
- [39] X. Zhuang, Y. Wan, C. Feng, Y. Shen, D. Zhao, Highly efficient adsorption of bulky dye molecules in wastewater on ordered mesoporous carbons, *Chem. Mater.* 21 (2009) 706–716.
- [40] V. Vadivelan, K.V. Kumar, Equilibrium, kinetics, mechanism, and process design for the sorption of methylene blue onto rice husk, *J. Colloid Interface Sci.* 286 (2005) 90–100.
- [41] L.R. Radovic, I.F. Silva, J.I. Ume, J.A. Menéndez, C. León y León, A.W. Scaroni, An experimental and theoretical study of the adsorption of aromatics possessing electron-withdrawing and electron-donating functional groups by chemically modified activated carbons, *Carbon*, 35 (1997) 1339–1348.
- [42] C. Moreno-Castilla, Adsorption of organic molecules from aqueous solutions on carbon materials, *Carbon* 42 (2004) 83–94.
- [43] M. Aschi, F. Mazza, A. Di Nola, Cation pi-interactions between ammonium ion and aromatic rings: An energy decomposition study, *J. Mol. Struct.* 587 (2002) 177–188.
- [44] M.A.M. Khraisheh, M.A. Al-Ghouti, S.J. Allen, M.N. Ahmad, Effect of OH and silanol groups in the removal of dyes from aqueous solution using diatomite, *Water Res.* 39 (2005) 922–932.
- [45] P. Liao, S. Yuan, W. Zhang, M. Tong, K. Wang, Mechanistic aspects of nitrogen-heterocyclic compound adsorption on bamboo charcoal, *J. Colloid Interface Sci.* 382 (2012) 74–81.